ELSEVIER

Chemical Engineering Journal 119 (2006) 19–26

Chemical Engineering Journal

www.elsevier.com/locate/cej

Mathematical models for macro-scale mass transfer in airlift loop reactors

Tongwang Zhang, Bin Zhao, Jinfu Wang *

Beijing Key Lab of Green Reaction Engineering and Technology, Tsinghua University, Beijing 100084, China

Received 18 May 2005; received in revised form 6 March 2006; accepted 9 March 2006

Abstract

Inter-phase mass transfer is an important issue for design and development of airlift loop reactors of high performance in either chemical or biochemical applications. In this work, the axial dispersion in both gas and liquid phases was taken into account for modeling the macro-scale mass transfer in airlift loop reactors. Finite difference method was used to numerically solve the differential equation system of the mass transfer model. For oxygen, the numerical results showed that the solute concentration of the gas phase can be treated as constant and the flow pattern of the liquid phase as a plug flow. Based on the conclusion obtained from numerical solution, the mass transfer model was simplified and the analytical solution of the simplified model was obtained. Comparison between the numerical and analytical solutions showed that the simplification of the model was reasonable and there was almost no influence on the calculated results. Experimental measurements on the mass transfer rate were carried out to verify the mathematical model. The comparison between the experimental and calculated results showed that the mass transfer model has satisfactory prediction ability and can be used to describe the mass transfer process in airlift loop reactors.

Keywords: Airlift loop reactor; Mass transfer; Axial dispersion model

1. Introduction

Airlift loop reactors have emerged as one of the most promising devices in chemical, biochemical and environmental engineering operations. Its main advantages over conventional reactors include excellent contact among the gas–liquid–solid phases, ease of removal or replenishment of solids, and high heat and mass transfer rates [1,2]. A high gas–liquid contacting area and a favorable flow pattern are the attractive properties of this type of three-phase contactors. Typical processes that can use this type of reactor include synthesis of methanol or dimethyl ether from syngas, coal liquefaction, Fischer–Tropsch synthesis and petroleum refining [3].

Inter-phase mass transfer is an important issue in development and design of airlift loop reactors with high performance for either chemical or biochemical applications. Multiphase reactors require efficient mixing and high mass transfer rate in order to achieve a better performance for chemical reaction. Airlift loop reactors have been proven to be able to realize high mass transfer rate and efficient mixing [4,5]. Most researchers focused on the investigation of volumetric mass transfer coefficient under different operation conditions [6–8] or the profile of solute concentration [9]. Only a few researchers investigated the dynamic mass transfer process [10,11]. Korpijarvi et al. [11] applied the axial dispersion equation to the gas and liquid phases in an airlift loop reactor. A general model consisting of a set of partial different equation was established. Because their reactor was not tall enough, they did not find the evolution of oxygen concentration should be a staircase curve [10]. Dhaouadi et al. [12] established a simple model under the assumption that liquid flow in the riser and down-comer are plug flow and the oxygen concentration in gas phase is constant. Even though this model can explain the dynamic mass transfer process, the reason that the general model can be simplified with such assumptions had not been proved. For such gases with low solubility as oxygen and nitrogen, it is correct to regard the solute concentration as constant. However, this assumption is incorrect for gases with high solubility, such as chlorine hydride and ammonia. Therefore, it is important to study when the solute in gas phase can be regarded as constant.

Airlift loop reactors were regarded as continuous stirred tank reactors when calculating the mass transfer coefficient [4,13]. However, there was no verification about the validation of these simplifications for the macro-scale mass transfer models [14]. Therefore, it is of significance to ascertain the behavior of different mass transfer models and establish practical and simple

* Corresponding author. Tel.: +86 10 62785464; fax: +86 10 62772051.
E-mail address: wangjf@flotu.org (J. Wang).

1385-8947/$ – see front matter © 2006 Elsevier B.V. All rights reserved.
doi:10.1016/j.cej.2006.03.005

Nomenclature

a	cross-sectional area (m^2)
C	oxygen concentration (mol/m^3)
E	dispersion coefficient (m^2/s)
h	reactor height (m)
H	Henry's constant (m^3/mol)
k	mass transfer coefficient (m^2/s)
p	pressure (Pa)
t	time in Lagrange coordinate (s)
u	velocity (m/s)
U	superficial velocity (m/s)
x	Eulerian axial coordinate (m)

Subscripts

D	time delay
G	gas
L	liquid

Greek symbols

ε	gas holdup
ξ	Lagrange axial coordinate (m)
τ	time in Lagrange coordinate (s)

models to describe the dynamic mass transfer process in airlift loop reactors. Because the airlift loop reactor was often used as bioreactor in the early time, air was often used as the gas phase. In most literature, oxygen mass transfer coefficient was used to represent the mass transfer ability of an airlift loop reactor [11,15]. So in this paper, air is regard as the gas phase and oxygen as the solute.

In the present paper, axial dispersion equation was applied to the gas and liquid phase in the riser and inter-phase mass transfer was source terms for the two equations. A general mass transfer model was established and the model consisted of a set of partial different equations. On the basis of the numerical results, it was shown that the liquid flow in the riser can be regarded as a plug flow and the solute in gas phase due to inter-phase mass transfer is negligible. The general model was simplified to give a simple model. Then an analytical solution was obtained in the Lagrange coordinate. The numerical solution of the general model was compared with the analytical solution of the simplified model. They showed less difference and their trends reaching the saturated concentration were similar. The analytical solution was also verified by the experimental measurements under consideration of the response delay of the oxygen sensor. The results proved that the simplified model can be used to describe the evolution of the oxygen concentration in airlift loop reactors.

2. Macro-scale mass transfer models

2.1. General model

Due to the agitation of bubbles and liquid back-mixing, the flow in the riser was modeled with a axial dispersion model [10]. The existence of the separator was considered as a prolongation of the riser [12]. Because there are few bubbles in the down-comer, the flow in it was considered as a plug flow. The stream in the down-comer only possesses a pure time delay, τ_D, therefore, there is no inter-phase mass transfer there. The oxygen concentration at the exit of the down-comer is the oxygen concentration at the entrance of the down-comer after τ_D. The axial dispersion model is applied for the liquid and gas phases in the riser to set up the mass transfer model. For internal-loop airlift reactor, bubbles were entrained into the down-comer and there was inter-phase mass transfer in the down-comer. τ_D should be replaced by an axial dispersion equation of the down-comer, which does not make the model more complicated. The control equations of mass transfer in the riser can be written as [16]:

$$\frac{\partial C_L}{\partial t} = E_L \frac{\partial^2 C_L}{\partial x^2} - \frac{U_L}{1-\varepsilon}\frac{\partial C_L}{\partial x} + \frac{1}{1-\varepsilon}k_L a\left(\frac{C_G}{H} - C_L\right) \quad (1)$$

$$\frac{\partial C_G}{\partial t} = E_G \frac{\partial^2 C_G}{\partial x^2} - \frac{U_G}{\varepsilon}\frac{\partial C_G}{\partial x} - \frac{1}{\varepsilon}k_L a\left(\frac{C_G}{H} - C_L\right) \quad (2)$$

These partial differential equations should be complemented with initial conditions:

$$C_L(x,0) = 0, \qquad C_G(x,0) = 0 \quad (3)$$

and boundary conditions:

$$C_L(0, t+\tau_D) = C_L(h,t), \qquad C_G(0,t) = C_G^* \quad (4)$$

$$x = h: \quad \frac{dC_L}{dx} = 0; \qquad \frac{dC_G}{dx} = 0 \quad (5)$$

Here C_G^* is the oxygen concentration in gas phase at the entrance of the riser.

2.2. Numerical solution of the general model

The macro-scale mass transfer model of an airlift loop reactor consists of a set of partial differential equations. The presence of advection terms and source terms in Eqs. (1) and (2) makes the differential equations difficult to be solved analytically. Hence numerical methods have to be used to solve the partial differential equation set. The upwind scheme was used to the advection terms and the central difference scheme to the dispersion terms [17]. Difference equations of the mass transfer model can be obtained after discretization treatment as follows:

$$\frac{C_{L,i}^n - C_{L,i}^{n-1}}{\Delta t} = E_L \frac{C_{L,i+1}^n - 2C_{L,i}^n + C_{L,i-1}^n}{\Delta x^2} - \frac{U_L}{1-\varepsilon}\frac{C_{L,i+1}^n - C_{L,i-1}^n}{2\Delta x} + \frac{1}{1-\varepsilon}k_L a\left(\frac{C_{G,i}^{n-1}}{H} - C_{L,i}^{n-1}\right) \quad (6)$$

Table 1
Parameters needed in the model

h (m)	4
U_L (m/s)	1
H (m^3/mol)	1.8228×10^6
T (K)	298.15
k_La (s^{-1})	0.1
U_G (m/s)	0.08
C_{G0} (mol/m^3)	9.5662
E_L (m^2/s)	0.1
E_G (m^2/s)	0.01
ε_G	0.06

$$\frac{C_{G,i}^n - C_{G,i}^{n-1}}{\Delta t} = E_G \frac{C_{G,i+1}^n - 2C_{G,i}^n + C_{G,i-1}^n}{\Delta x^2} - \frac{U_G}{\varepsilon} \frac{C_{G,i+1}^n - C_{G,i-1}^n}{2\Delta x} - \frac{1}{\varepsilon} k_L a \left(\frac{C_{G,i}^{n-1}}{H} - C_{L,i}^{n-1} \right) \quad (7)$$

The following abbreviations are introduced:

$$\mu_L = \frac{E_L \Delta t}{\Delta x^2}, \qquad \lambda_L = \frac{U_L \Delta t}{2(1-\varepsilon)\Delta x}, \qquad \beta_L = \frac{k_L a}{1-\varepsilon} \quad (8)$$

$$\mu_G = \frac{E_G \Delta t}{\Delta x^2}, \qquad \lambda_G = \frac{U_G \Delta t}{2(1-\varepsilon)\Delta x}, \qquad \beta_G = \frac{k_L a}{\varepsilon} \quad (9)$$

Then Eqs. (6) and (7) are shown as follows:

$$(-\mu_L - \lambda_L) C_{L,i-1}^n + (1 + 2\mu_L) C_{L,i}^n + (-\mu_L + \lambda_G) C_{L,i+1}^n = (1 - \beta_L) C_{L,i}^{n-1} + \beta_L \frac{C_{G,i}^{n-1}}{H} \quad (10)$$

$$(-\mu_G - \lambda_G) C_{G,i-1}^n + (1 + 2\mu_G) C_{G,i}^n + (-\mu_G + \lambda_G) C_{G,i+1}^n = (1 - \beta_G) \frac{C_{G,i}^{n-1}}{H} + \beta_G C_{L,i}^{n-1} \quad (11)$$

The boundary conditions at the exit of the riser are discretized as:

$$C_{L,i}^n = C_{L,i}^{n-1} - 2\lambda_L (C_{L,i}^{n-1} - C_{L,i-1}^{n-1}) + \beta_L \left(\frac{C_{G,i-1}^{n-1}}{H} - C_{L,i}^{n-1} \right) \quad (12)$$

$$C_{G,i}^n = C_{G,i}^{n-1} - 2\lambda_G (C_{G,i}^{n-1} - C_{G,i-1}^{n-1}) - \beta_G \left(\frac{C_{G,i-1}^{n-1}}{H} - C_{L,i}^{n-1} \right) \quad (13)$$

The parameters needed are given in Table 1. Henry constant was obtained from physical chemistry manual and others were determined based on the experimental measurements. Liquid velocity and gas holdup can be measured experimentally. All the parameters are in the range of the data in literatures [18,19]. This is a hypothetical experiment. From the numerical result of the hypothesis experiment, the conclusion for simplifying the general model is obtained.

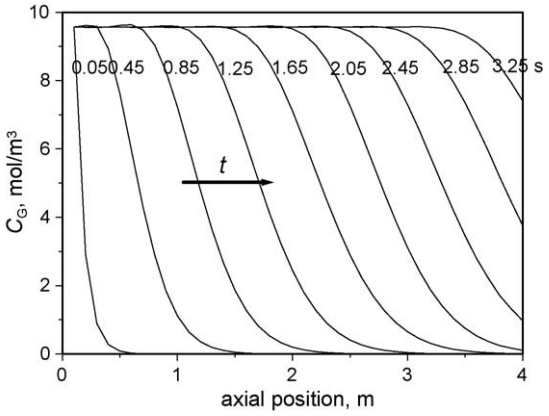

Fig. 1. The axial profile evolution of oxygen concentration in gas phase.

Fig. 1 shows the axial profile of oxygen concentration of the gas phase in the riser at different time obtained from the numerical solution. The step change of the oxygen concentration in the gas phase moves from the entrance to the exit of the riser. And the steep leading edge becomes more and more smooth along the upward flow due to the gas phase dispersion. Even though there exist axial dispersion and inter-phase mass transfer in gas phase, the oxygen concentration in the gas phase is almost constant because the consumed oxygen amount due to inter-phase mass transfer is much less than its total amount. Therefore, the oxygen concentration of the gas phase in the riser almost keeps constant after the leading edge. And the oxygen concentration will keep constant in the whole riser when the step edge of the oxygen concentration of gas phase reaches the exit of the riser.

Fig. 2 shows the axial profile of oxygen concentration of the liquid phase in the riser under a time interval of 1 s. The oxygen concentration evolves wavelike due to the liquid circulation and the wave peak becomes flatter and flatter with the liquid circulation. The oxygen concentration in liquid phase increases gradually. Even though there exists axial dispersion, the distribution of oxygen concentration in axial direction is distinct.

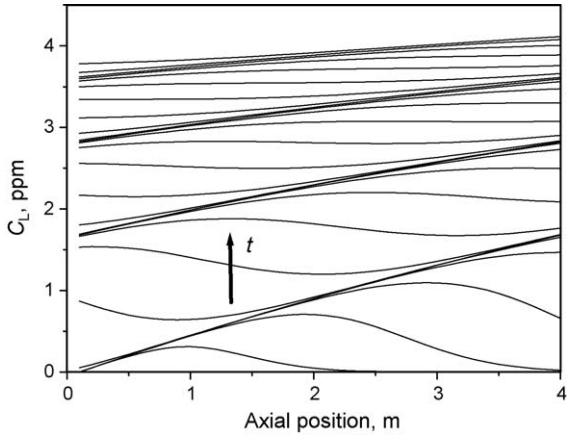

Fig. 2. The axial profile evolution of oxygen concentration in liquid phase.

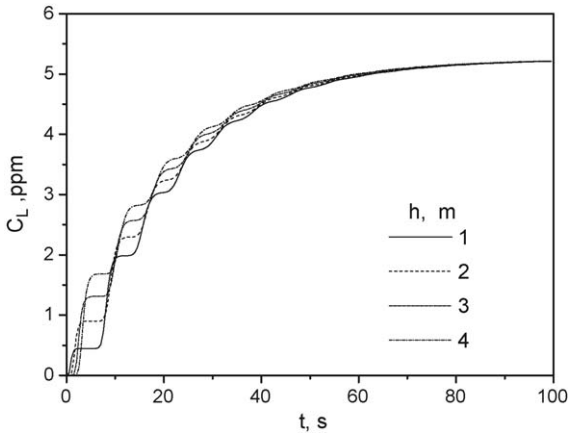

Fig. 3. Evolution of oxygen concentration obtained from the general model.

This shows that the model can be simplified by neglecting the dispersion terms. The evolutions of oxygen concentration in liquid phase at different axial positions are staircase curves, as illustrated in Fig. 3. The oxygen concentration increases rapidly at the beginning, and then reaches *andante* the saturated concentration. Because of the existence of time delay in the down-comer, there are some stagnations of oxygen concentration during its evolution and the evolution is staircase curve. Similar result had also obtained by Dhaouadi et al. experimentally [10].

2.3. Simplified model

As shown in Figs. 1 and 2, the axial dispersion has no remarkable influence on the profile of oxygen concentration in liquid phase and the assumption of oxygen in gas phase can be negligible. Therefore, the oxygen concentration in gas phase at one axial position, x, can be regarded as constant when $t > x/u_G$ and the dispersion term can be ignored. Both the liquid flows in the riser and down-comer are considered as plug flow. Hence Eqs. (1) and (2) can be reduced to one partial differential equation:

$$\frac{\partial C_L}{\partial t} + u_L \frac{\partial C_L}{\partial x} = k\left(\frac{C_G}{H} - C_L\right) \tag{14}$$

And u_L and k are determined from U_L and ε as:

$$u_L = \frac{U_L}{1-\varepsilon}, \qquad k = \frac{k_L a}{1-\varepsilon} \tag{15}$$

The initial conditions, Eq. (3), and boundary conditions, Eq. (4), are also used here. The oxygen concentration at the top of the riser is the concentration at the bottom of the riser after time delay, τ_D.

When the reactor is high enough, the changes in gas phase oxygen concentration will have effect on dynamic mass transfer process when the reactor is high enough. The effect of static hydrodynamic pressure effect on the solute concentration in gas phase was taken into account. The pressure at the column bottom was taken as the reference. Because the assumption of oxygen in gas phase can be negligible, the gas phase oxygen concentration is proportional to the static pressure:

$$p(x) = p(0) - (p(0) - p(h))\frac{x}{h} \tag{16}$$

$$C_G(x) = C_{G0}\frac{p(x)}{p(0)} \tag{17}$$

$$a = \frac{1 - p(h)/p(0)}{h} \tag{18}$$

$$C_G(x) = C_{G0}(1 - ax) \tag{19}$$

where $p(x)$ is the pressure at the axial position, x.

For internal-loop airlift reactor, there is mass transfer in the down-comer. Axial dispersion model with source term should be applied to the down-comer. The simplification process is similar to the previous derivation and the process to solve it is similar to the following method by using coordinate transform.

2.4. Analytical solution of the simplified model

Eq. (14) was set up in the Eulerian coordinate. Laplace transform has been used to solve this partial differential equation in literature [12]. However, the solution procedure is very cumbersome and the result is also a complexity. Because of the neglect of dispersion term, we can focus on an infinitesimal fluid element that flows at a velocity of u_L. The axial position of the fluid element is ξ at time τ_0. The Eulerian coordinate can be transformed to Lagrange coordinate by a coordinate transformation. Then the advection term in Eq. (14) disappears and the partial differential equation becomes an ordinary differential equation as following:

$$\frac{dC_L(\xi,\tau)}{d\tau} = k(C_L^0(1 - a\xi - au\tau) - C_L(\xi,\tau)) \tag{20}$$

$$x = \xi + u_L\tau \tag{21}$$

$$t = \tau + \tau_0 \tag{22}$$

$$C_L^0 = \frac{C_G^*}{H} \tag{23}$$

The analytical solution of Eq. (20) can be obtained easily and reads:

$$C_L(\xi,\tau) = C_L^0(1 - a\xi) - C_L^0 au\tau + \frac{C_L^0 au}{k} + F(\xi)\exp(-k\tau) \tag{24}$$

$$F(\xi) = C_L(\xi,\tau_0) - C_L^0(1 - a\xi) - \frac{C_L^0 au}{k} \tag{25}$$

Eq. (24) showed the evolution of oxygen concentration in an infinitesimal fluid element moving at the velocity u_L from the axial position, ξ, at time τ_0. If we assume that the fluid element locates at $\xi = 0$ when $\tau_0 = 0$, and then it will move to $x = u_L t$ when $\tau = t$. According to this relationship, the concentration at (x, t) can be determined by the concentration at $(0, t - x/u)$ and the time delay, x/u. In this way, the coordinate can be transformed

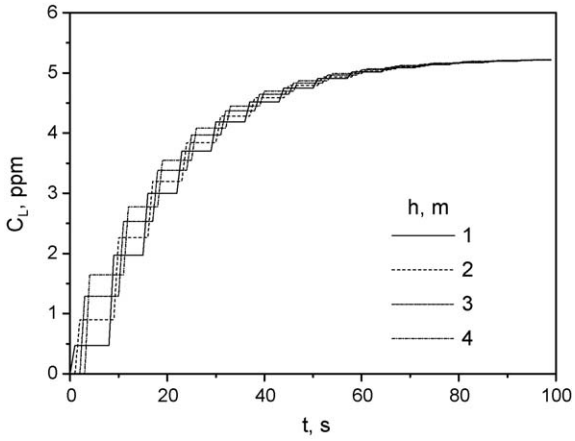

Fig. 4. Evolution of oxygen concentration obtained from the simplified model.

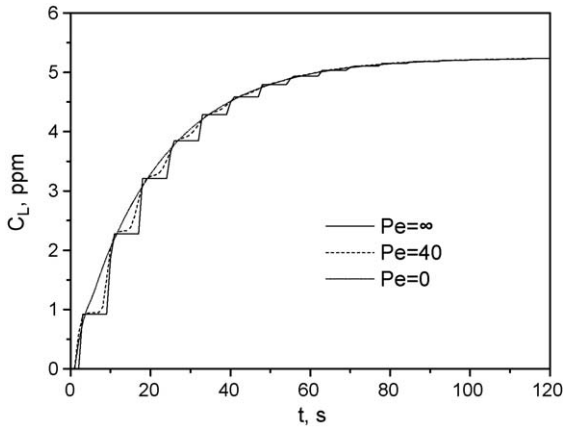

Fig. 5. Influence of Peclet number on the mass transfer behavior.

back from Lagrange to Eulerian coordinate and Eq. (24) can be presented as:

$$C_{\mathrm{L}}(x,t) = C_{\mathrm{L}}^0 - C_{\mathrm{L}}^0 ax + \frac{C_{\mathrm{L}}^0 au}{k} + \left(C_{\mathrm{L}}\left(0, t-\frac{x}{u}\right) - C_{\mathrm{L}}^0 - \frac{C_{\mathrm{L}}^0 au}{k}\right)\exp\left(-k\frac{x}{u}\right) \tag{26}$$

The oxygen concentration at the exit of the riser can be obtained from Eq. (26) by substituting x with h:

$$C_{\mathrm{L}}(h,t) = C_{\mathrm{L}}^0 - C_{\mathrm{L}}^0 ah + \frac{C_{\mathrm{L}}^0 au}{k} + \left(C_{\mathrm{L}}\left(0, t-\frac{h}{u}\right) - C_{\mathrm{L}}^0 - \frac{C_{\mathrm{L}}^0 au}{k}\right)\exp\left(-k\frac{h}{u}\right) \tag{27}$$

Combining Eqs. (4) and (27), the liquid concentration at the riser entrance can be expressed in a function of time as:

$$C_{\mathrm{L}}(0, t+\tau_{\mathrm{D}}) = C_{\mathrm{L}}^0 - C_{\mathrm{L}}^0 ah + \frac{C_{\mathrm{L}}^0 au}{k} + \left(C_{\mathrm{L}}\left(0, t-\frac{h}{u}\right) - C_{\mathrm{L}}^0 - \frac{C_{\mathrm{L}}^0 au}{k}\right)\exp\left(-k\frac{h}{u}\right) \tag{28}$$

Eq. (28) is equivalent to the following equation:

$$C_{\mathrm{L}}(0,t) = C_{\mathrm{L}}^0 - C_{\mathrm{L}}^0 ah + \frac{C_{\mathrm{L}}^0 au}{k} + \left(C_{\mathrm{L}}\left(0, t-\frac{h}{u}-\tau_{\mathrm{D}}\right) - C_{\mathrm{L}}^0 - \frac{C_{\mathrm{L}}^0 au}{k}\right)\exp\left(-k\frac{h}{u}\right) \tag{29}$$

When $t < h/u_{\mathrm{G}} + \tau_{\mathrm{D}}$, the concentration at the entrance of the riser is zero. And when $h/u_{\mathrm{G}} + \tau_{\mathrm{D}} t < h/u_{\mathrm{L}} + \tau_{\mathrm{D}}$, the concentration follows an exponential function. That is:

$$C_{\mathrm{L}}(0,t) = \begin{cases} 0, & t \le \dfrac{h}{u_{\mathrm{G}}} + \tau_{\mathrm{D}} \\ C_{\mathrm{L}}^0\left[1 - \exp\left(\dfrac{(u_{\mathrm{G}}t - h)k}{u_{\mathrm{G}} - u_{\mathrm{L}}}\right)\right], & \dfrac{h}{u_{\mathrm{G}}} + \tau_{\mathrm{D}} < t \le \dfrac{h}{u_{\mathrm{L}}} + \tau_{\mathrm{D}} \end{cases} \tag{30}$$

Then the liquid concentration at any axial positions in the riser can be calculated from Eqs. (26) and (29).

The parameters used in the simplified model are the same as those in Table 1. Fig. 4 presents the evolution of oxygen concentration of the liquid phase at different axial positions. Similar to Fig. 3, the oxygen concentration increases rapidly at the beginning, and then reaches *andante* the saturated concentration. Because of ignoring the dispersion in the riser, the stagnations of oxygen concentration from the simplified model are more abrupt here. The step change will become less and less and approach exponential increase by and by with increasing liquid velocity. Because of the time delay of the dissolved oxygen sensor, the experimental data would be a smooth curve at high liquid velocity.

3. Comparison of the models

Fig. 5 presents the evolution of oxygen concentration under different Peclet numbers. The dash line, $Pe = 40$, represents the results of the numerical solution from the general model under the conditions listed in Table 1 and the solid line, $Pe = \infty$, represents the results of the analytical solution from the simplified model. The difference between the dash line and solid is very less. This shows that the analytical solution can approach the numerical solution very well at large Peclet number. The short dot line, $Pe = 0$, is drawn based on the assumption that the riser is

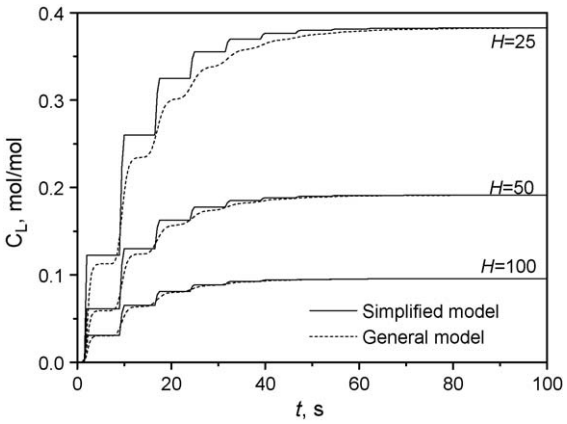

Fig. 6. Comparison of the numerical solution from the general model to the analytical solution from the simplified model under different Henry's constants.

considered as continuous stirred tank reactor. Fig. 5 shows that the step changes become more and more smooth with decreasing Peclet number. But the trend that it reaches the saturated oxygen concentration is coincident. As reported by literatures, Peclet number is larger than 40 [20–22], so the analytical solution can be used to substitute the numerical solution in reality. During measuring the dissolved oxygen in the liquid phase, the sensor response coefficient smoothes the step change and weakens the effect of dispersion. This would further reduce the difference between these two models and made the simplified model coincided with the experimental data.

If the mass transfer coefficient is large enough or the Henry number is little enough, the inter-phase mass transfer process would influence the solute concentration in the gas phase remarkably. This would lead to the fact that the solute concentration in the gas phase cannot be regarded as constant. And the analytical solution of the simplified model would not coincide with the numerical solution of the general model in this case. Therefore, it is important to investigate the influence of the solute's solubility on the mass transfer process. Because the volumetric mass transfer coefficient, k_La, is usually less than $0.4\,s^{-1}$ in gas–liquid or gas–liquid–solid systems [6,7,23,24], the influence of Henry number is investigated in the case of $k_La = 0.4\,s^{-1}$. Fig. 6 compared the evolution of oxygen concentration under different Henry numbers. The results show that the analytical solution can substitute the numerical solution even though the Henry number takes a very small value such as $100\,m^3/mol$.

4. Model verification

Experiments were carried out in an airlift external-loop reactor with a height of 3.5 m, as shown in Fig. 7. The diameter of the riser and down-comer are 100 mm. Tap water was used as liquid phase for the experiments and the feed of gas phase could be switched from air to nitrogen or vice versa. The oxygen concentrations were measured at a position of 3 m above the gas distributor in the riser by Galvanic cell type oxygen sensor connected to a data-acquisition system.

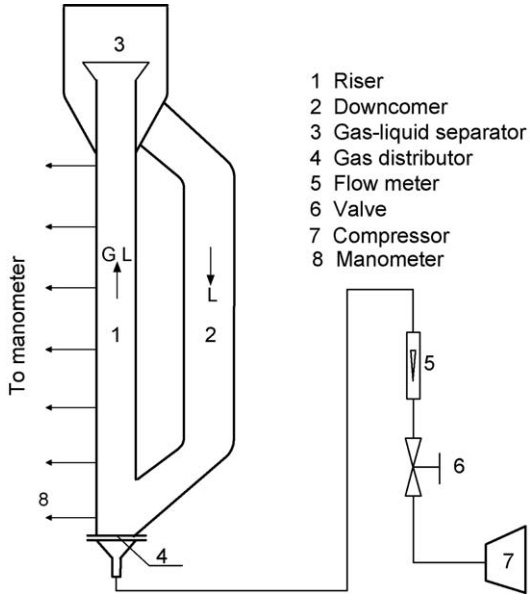

Fig. 7. The schematic diagram of the experimental apparatus.

The well-known transient gassing-in (or gassing-out) technique [25] was employed for the determination of the overall volumetric mass transfer coefficient (k_La): a batch of liquid (or slurry) was deaerated to a low oxygen concentration by bubbling nitrogen. The nitrogen supply was then switched to air feed into the riser with a pre-set value. The time-change in dissolved oxygen (DO) in the reactor was monitored from the time point at which the air-flow began.

An ultrasonic Doppler velocimetry was used to measure the liquid velocity, u_L [26]. Gas holdup in the riser of the airlift loop reactor was determined by measuring the hydrodynamic pressure differences with invert U-tube manometers. And the time delay τ_D was then obtained from the liquid velocity, u_L, and the down-comer height h. The experimental sensor response coefficient, k_p, took a value of 0.125 s which was determined by a classical concentration switch method [19]. The volumetric mass transfer coefficient, k_La, was determined by sensitivity analysis based on the experimental measured data.

The experimental data measured by the sensor is influenced not only by the oxygen concentration in the liquid phase, but also by the sensor response coefficient, k_p. In order to verify the simplified model, the analytical solution based on the parameters mentioned previously had to convolute with the following equation:

$$\Gamma(t) = k_p \exp(-k_p t) \tag{31}$$

Fig. 8 illustrates the comparison between the calculated results from the simplified model, shown by lines, and the experimental measured results, shown by different symbols. The liquid velocity was obtained by ultrasonic velocimeter [26]. The volumetric mass transfer coefficients, k_La, were obtained from experiments by sensitivity analysis under different operating conditions [10,11], as shown in Fig. 8. By taking into account the sensor response coefficient [27], even through the axial dispersion is ignored in the simplified model, the simplified model

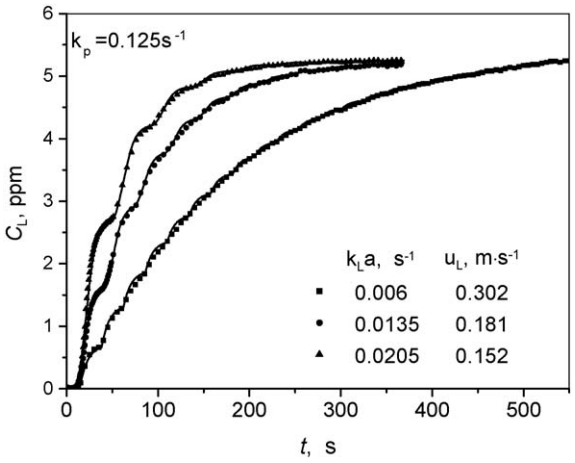

Fig. 8. Comparison between the experimental and calculated results under different operating conditions: curves, calculated; symbols, experimental measured.

can still satisfactorily describe the mass transfer process in the airlift loop reactor in detail. The analytical results from the mass transfer model for the airlift loop reactor agree well with the experimental measurements. This shows that the simplified model is reasonable and can be used to predict the axial profile of oxygen concentration and the evolution of oxygen concentration at certain positions in the riser.

5. Conclusions

A mass transfer model was established for airlift loop reactors based on the axial dispersion model for the gas and liquid phases, respectively. The proposed model was a set of partial differential equations that can only be solved by using finite difference method numerically. The numerical results from the general mass transfer model showed that the oxygen concentration of the gas phase in the riser can be regarded as constant and the liquid flow can be considered as plug flow.

Based on the numerical results, the general mass transfer model was simplified by assuming a constant oxygen concentration in the gas phase and ignoring the axial dispersion in the liquid phase. The simplified model was solved analytically by using a method of coordinate transform from Eulerian to Lagrange coordinate. Comparison between the numerical and analytical solutions showed that the simplified model can substitute for the general model for most conditions. Experimental measurements were carried out to verify the mathematical model for describing the mass transfer process in airlift loop reactors. The comparison between the experimental and simulated results showed that the mass transfer model is reasonable and can be used to predict the process of mass transfer in airlift loop reactors.

Acknowledgements

The authors gratefully acknowledge the financial supports by the National Natural Science Foundation of China (No. 20576060) and Specialized Research Fund for the Doctoral Program of Higher Education (No. 20050003030).

References

[1] M.H. Siegel, C.W. Robinson, Applications of airlift gas–liquid–solid reaction in biotechnology, Chem. Eng. Sci. 47 (13/14) (1992) 3215–3229.
[2] W.A. Al-Masry, Influence of gas separator and scale-up on the hydrodynamic of external-loop circulating bubble columns, Chem. Eng. Res. Des. 82 (part A) (2004) 381–389.
[3] K.H. Choi, Y. Chisti, M. Moo-Young, Comparative evaluation of hydrodynamic and gas–liquid mass transfer characteristics in bubble column and airlift slurry reactors, Chem. Eng. J. 62 (1996) 223–229.
[4] M.Y. Chisti, Airlift Bioreactors, Elsevier Applied Science, New York, 1989.
[5] K.H. Choi, Y. Chisti, M. Moo-Young, Influence of the gas–liquid separator design on hydrodynamic and mass transfer performance of split-channel airlift reactors, J. Chem. Technol. Biotechnol. 62 (4) (1995) 327–332.
[6] G. Olivieri, A. Marzocchella, P. Salatino, Hydrodynamics and mass transfer in a lab-scale three-phase internal-loop airlift, Chem. Eng. J. 96 (2003) 45–54.
[7] A. Fadavi, Y. Chisti, Gas–liquid mass transfer in a novel forced circulation loop reactor, Chem. Eng. J. 112 (1–3) (2005) 73–80.
[8] A. Couvert, D. Bastoul, M. Roustan, et al., Hydrodynamic and mass transfer study in a rectangular three-phase airlift loop reactor, Chem. Eng. Process. 43 (2004) 1381–1387.
[9] E. Camarasa, L.A.C. Meleiro, E. Carvalho, et al., A complete model for oxidation air-lift reactors, Comput. Chem. Eng. 25 (2001) 577–584.
[10] H. Dhaouadi, S. Poncin, J.M. Hornut, et al., Mass transfer in an external-loop airlift reactor: experiments and modeling, Chem. Eng. Sci. 52 (21) (1997) 3909–3918.
[11] J. Korpijarvi, P. Oinas, J. Reunanen, Hydrodynamics and mass transfer in an airlift reactor, Chem. Eng. Sci. 54 (13/14) (1999) 2255–2262.
[12] H. Dhaouadi, S. Poncin, N. Midoux, et al., Gas–liquid mass transfer in an airlift reactor-analytical solution and experimental confirmation, Chem. Eng. Process. 40 (2001) 129–133.
[13] V. Linek, J. Sinkule, The influence of gas and liquid axial-dispersion on determination of k_La by dynamic method, Chem. Eng. Res. Des. 69 (1991) 308–312.
[14] M. Blazej, J. Annus, J. Markos, Comparison of gassing-out and pressure-step dunamic methods for k_La measurement in an airlift reactor with internal loop, Chem. Eng. Res. Des. 82 (A10) (2004) 1375–1382.
[15] M. Tobajas, E. Garcia-Calvo, M.H. Siegel, et al., Hydrodynamics and mass transfer prediction in a three-phase airlift reactor for marine sediment biotreatment, Chem. Eng. Sci. 54 (1) (1999) 5347–5354.
[16] O. Levenspiel, Chemical Reaction Engineering, Wiley, New York, 1999.
[17] W.F. Ames, Numerical Methods for Partial Differential Equations, Academic Press, 1977.
[18] T.W. Zhang, J.F. Wang, Z. Luo, et al., Multiphase flow characteristics of a novel internal-loop airlift reactor, Chem. Eng. J. 109 (1) (2005) 115–122.
[19] C. Freitas, J.A. Teixeira, Oxygen mass transfer in a high solids loading three-phase internal-loop airlift reactor, Chem. Eng. J. 84 (1) (2001) 57–61.
[20] G.Q. Yang, L.S. Fan, Axial liquid mixing in high-pressure bubble columns, AIChE J. 49 (8) (2003) 1995–2208.
[21] G. Maria, Z.T. Radu, Mixing studies in external-loop airlift reactors, Chem. Eng. J. 66 (1997) 97–104.
[22] A.S. Miron, M.-C.C. Garcia, F.G. Camacho, et al., Mixing in bubble column and airlift reactors, Chem. Eng. Res. Des. 82 (10) (2004) 1367–1374.
[23] L.S. Fan, Gas–liquid–solid Fluidization Engineering, Butterworths, Boston, 1989.

[24] R.A. Bello, C.W. Robinson, M. Moo-Young, Gas holdup and overall volumetric oxygen transfer coefficient in airlift contactors, Biotechnol. Bioeng. 27 (3) (1985) 369–381.

[25] Y.X. Guo, M.N. Rathor, H.C. Ti, Hydrodynamics and mass transfer studies in a novel external-loop airlift reactor, Chem. Eng. J. 67 (1997) 205–214.

[26] T.F. Wang, J.F. Wang, Y. Jin, Application of Doppler ultrasound velocimetry in multiphase flow, Chem. Eng. J. 92 (2003) 111–122.

[27] K. Van't Riet, Review of measuring methods and results in nonviscous gas–liquid mass transfer in stirred vessels, Ind. Eng. Chem. Process. Des. Develop. 18 (3) (1979) 357–364.